

Contents list available at CBIORE journal website

International Journal of Renewable Energy Development

Journal homepage: https://ijred.cbiore.id



Research Article

Aluminum, nickel, and manganese supported on bentonite for conversion of ethanol to gasoline

Deri Rahmanda[®], Sri Wardhani[®], Ulfa Andayani[®], Robert R. Widjaya^{b*}, Adid A. Dwiatmoko[®], Nino Rinaldi[®], Joni Prasetyo[®], Kezia F. Kurniawan[®]

Abstract. The potential of bentonite as a catalyst is rapidly growing, isomorphic substitution in its interlayer allows for cation exchange and facilitates modification to enhance its catalytic properties. The catalytic performance of bentonite can be improved through the insertion of pillared clays (PILC) into its interlayer structure using Al_2O_3 , NiO, and MnO metal oxide alloys. This research aims to develop and study a modified bentonite catalyst, focusing on its physicochemical changes, as well as its activity and selectivity in the conversion of ethanol to biogasoline. The synthesis of oxide pillars on bentonite was carried out at a consistent metal/bentonite mole ratio of 10 mmol/g, with a mixed metal composition of 1:1. The results showed an expansion of interlayer distance, as measured by X-ray diffraction (XRD), which increased in all catalysts compared to natural bentonite 6.35° (13.94 Å). Surface Area Analyzer (SAA) analysis, revealed that Al/Bentonite exhibited the highest surface area at 187.84 m²/g. Total acidity analyzed, using Temperature Programmed Desorption-Ammonia (TPD-NH₃), was found to be 2.33 mmol/g, with Al-Ni/Bentonite showing the highest acidity. Thermal stability, tested through Thermogravimetric Analysis (TGA), indicated that catalysts containing Al and Ni demonstrated the highest stability. The catalytic activity test showed that the Al/bentonite catalyst achieved the highest ethanol conversion rate of 68.64% and a catalyst selectivity of 51.70%, as determined by Gas Chromatography-Flame Ionized Detector (GC-FID) analysis. These results indicate that the pillarization of bentonite with Al₂O₃, NiO, and MnO oxides significantly improved its physicochemical properties, activity, and selectivity in the catalytic conversion of ethanol to biogasoline compared to natural bentonite.

Keywords: Catalysis, Pillared Clay (PILC), Bimetallic oxide, Ethanol, Gasoline



@The author(s). Published by CBIORE. This is an open access article under the CC BY-SA license (http://creativecommons.org/licenses/by-sa/4.0/).

Received: 10th Nov 2024; Revised: 26th January 2025; Accepted: 20th Feb 2025; Available online: 27th Feb 2025

1. Introduction

The use of motorized vehicles is growing rapidly because it facilitates mobility. Most of these vehicles still rely on fossil fuels. The massive exploitation of fossil fuels has led to environmental damage, global warming, and harmful emissions resulting from the conversion of fossil fuel energy in motor vehicles. Goldemberg et al. (2007) reports that fossil fuels account for approximately 80% of the world's total energy supply. At the current rate of production and consumption, the world's known petroleum reserves are expected to last about 41 years, natural gas about 64 years, and coal about 155 years. Additionally, as reserves are depleted, production costs are predicted to rise due to the need for more expensive extraction technologies. The most viable alternative to fossil fuels is the development of renewable energy, particularly modern biomass. Currently, modern biomass accounts for only 1.91% of the total 3.40% renewable energy usage (Goldemberg, 2007). For this reason, it is necessary to develop the exploration of renewable energy* sources, one of which is the catalytic

conversion of ethanol to biogasoline (ETG/Ethanol to Gasoline).

Ethanol can be produced from plants or cellulose biomass materials through a fermentation process, resulting in an azeotropic bioethanol/ethanol-water mixture. Catalytic processes offer a direct alternative to using bioethanol without requiring an energy-intensive refining process. These processes facilitate the transformation of processed biomass into hydrocarbons, specifically by converting bioethanol into biogasoline (gasoline equivalent) (Rinaldi & Schüth, 2009). Systems that operate at lower energy costs, combined with the development of suitable catalysts from clay materials, can produce conversion products proven to be equivalent to fossil fuels. Ethanol has significant potential for development, as Indonesia possesses abundant natural resources and biomass for use as an energy source (Sun & Wang, 2014).

The use of catalysts in catalytic processes is an important parameter, as they increase the rate of chemical reactions without being consumed in the reaction. Clays are a type of heterogeneous catalyst and belong to the phyllosilicate or smectite class of minerals, characterized by a multilayered and

Department of Chemistry, Faculty of Mathematics and Natural Sciences, University of Brawijaya, Malang, Indonesia

 $[^]b$ Research Center for Chemistry, National Research and Innovation Agency, Kawasan PUSPIPTEK Serpong, South Tangerang, Indonesia

^cJakarta Intercultural School, Kota Jakarta Selatan, Daerah Khusus Ibukota Jakarta, Indonesia

^{*} Corresponding author Email: robeoo7@brin.go.id (R.R. Widjaya)

crystalline structure (Sun & Wang, 2014). In recent years, bentonite has gained particular attention as a catalyst. Bentonite mineral is one of Indonesia's abundant natural resources but is still rarely utilized optimally. Using bentonite as a catalyst has long been introduced, particularly in the petroleum cracking process. However, bentonite has low thermal stability due to dehydration, and fixed porosity. During the swelling and dehydration process, the bentonite layers become exposed, making chemical processes ineffective (Okoye & Obi, 2011). In addition, the ion exchange capability through the cation exchange mechanism offers potential for bentonite modification.

Naturally, bentonite can undergo an isomorphic substitution process, in which Mg^{2+} substitutes Al^{3+} in the octahedral layer, and Al^{3+} substitutes Si^{4+} in the tetrahedral layer. As a result, the natural clay layer acquires a negatively charge, although it remains relatively low (Widjaya *et al.*, 2012). The substitution of smaller charged ions $(Mg^{2+} \rightarrow Al^{3+}$ and $Al^{3+} \rightarrow Si^{4+})$ generates a negative charge on the structure, but most of it is balanced by the adsorbed interlayer cations (Kumar Dutta et al., 2015). Therefore, the unique catalytic properties of bentonite are of great interest and can be further optimized for various applications.

The catalytic performance of bentonite can be enhanced through the insertion of a pillaring agent composed of metal oxide polycations into its interlayer structure, forming pillared interlayer clay (PILC/pillared interlayer clay) (Okoye & Obi, 2011). The formation of oxide pillars as active components significantly influences the surface properties of bentonite. Therefore, pillarization optimizes the ratio of Lewis to Brønsted acid sites. In this study, using Al₂O₃, NiO and MnO₂ metal oxide alloys is highly feasible, as the interaction of various metals affects the morphology and particle size the morphology and particle size. A homogeneous distribution of metal oxides within the interlayer buffer occurs through strong chemical anchoring. This, in turn, determines the surface electronic properties and the nature of interactions between reactants and the active components of the catalyst (Fatimah et al., 2011).

The selection of metal oxides Al₂O₃, NiO and MnO₂ in this study is based on several factors, according to Widjaya, et al. (2012) Al₂O₃ oxide can increase basal spacing, enhance the microporous structure containing Lewis and Brønsted acid sites, and improve thermal stability at temperatures exceeding 500°C. Meanwhile, Mishra & Parida (1997) reported that MnO₂ enhances the specific surface area, which remains stable up to 500°C. Research conducted by Aid *et al.* (2017) demonstrated that NiO oxide-pillared clays with microporous and mesoporous structures exhibit a high specific surface area and hold significant potential for ethylene oligomerization reactions.

The use of catalysts with alloys of two metal oxides (bimetallic oxide pillars) in the ETG process is still rarely. In the research conducted by Ramadhaniati et al. (2023), the use of Al-Zr-PILC bimetallic oxide catalysts for the ETG process resulted in a higher conversion percentage compared to single-metal bentonite catalysts. The conversion products included n-Heptane, toluene, benzene, phenol, and n-hexane compounds which are direct components of commercial gasoline. Widjaya, et al. (2019), reported that using a Sn-Cr/bentonite bimetallic catalyst increased the basal spacing from 12.83 Å to 25.67 Å and the specific surface area of bentonite from 30.35 m²/g to 168.86 m²/g and the pore volume from 0.0065 cm³/g to 0.03 cm³/g. The catalytic process yielded gasoline components such as benzene, toluene, octane, and naphthalene, demonstrating that Sn-Cr/bentonite can be used as an ETG catalyst for engine fuel. Wijaya et al. (2021) also reported that the Ni/BZS catalyst (Nickel supported on acid-activated zirconia-pillared bentonite) produced a higher conversion percentage in biogasoline

products compared to BZ catalyst (zirconia-pillared bentonite). The use of a bimetallic alloy catalyst can enhance the catalyst's properties, including specific surface area and pore volume, thereby improving the results of the catalytic reaction test. This enhancement occurs because the two metals work synergistically, compensating for each other's strengths and weaknesses. In this reaction process, both Brønsted and Lewis acidity are required; therefore, incorporating two metals helps achieve a more optimal balance of these acidity types (Ramadhaniati *et al.*, 2023). The acidity value for single metal is usually limited and not higher than that of two metal alloy catalysts. The acidity will affect the cracking process of ethanol carbon chains into gasoline (Yanti *et al.*, 2020). Based on this background, bentonite catalysts pillared with bimetallic alloys have significant potential for enhancing catalytic activity.

2. Experiment

2.1 Catalyst preparation

Commercial bentonite was obtained from sigma aldrich (285234), Aluminum Chloride hexahydrate (AlCl₃.6H₂O) from Merck (1.01084.1000), Nickel (II) Chloride hexahydrate (NiCl₂.6H₂O) from Merck (1.06717.0250), and Manganese (II) Chloride tetrahydrate (MnCl₂.4H₂O)from (1.05927.0100). Metal alloy bentonite was synthesized by the pilarization method. The ratio of the degree of hydrolysis (OH-/mol of pillar metal) used was 2 with the concentration of pillar metal used being 0.1 M each and the concentration of NaOH solution being 0.2 M each. The pillar metal/bentonite ratio (mmol/g) was 10 and the bentonite base was 1% (5/500 g/mL). Mixed metal alloy bentonite was synthesized at 1:1 metal composition.

The synthesis was carried out by gradually dripping NaOH solution into each Al, Mn, Ni, Al-Mn, and Al-Ni metal solution under continuous stirring for 24 hours. A total of 5 g bentonite powder was dissolved in 500 mL pure water at 60° C for 2 hours. The homogenized metal hydroxide polycation solution was then added to the bentonite suspension with constant stirring for another 24 hours. The material was subsequently filtered and washed with distilled water at 60° C to neutralize Cl⁻ ions. The residue and filtrate were separated by centrifugation and the residue was dried in an oven at 80° C for 24 hours. The dried solid was then crushed until smooth and then calcinated using a furnace at 400° C for 4 hours.

2.2 Catalyst Characterization

The catalyst material was analyzed by X-ray diffraction (XRD) from Panalytical Varian AERIS using Cu-Kα, scan speed 2 deg/min, λ Cu 1.54 Å, radiation generated 40 kV, 15 mA, this aims to determine the interlayer distance in the reflected plane (d_{001}) and crystallinity so that the composition in the catalyst can be known according to the general crystal diffraction pattern. The distribution of metal oxides inserted on the interlayer and bentonite surface was measured by X-ray fluorescence (XRF) S2 PUMA from Brucker, under Helium gas flow. Fourier Transform Infra-Red (FTIR) type Tensor II from Bruker and using KBr phase method, prestige-21 with ATR 4000 connected to an automated data acquisition center, to ensure identification of functional groups and acidity points. Acidity analysis was performed using Temperature Programmed Desorption-Ammonia (TPD-NH₃) with a Micromeritics chemisorb 2750, the samples were heated at 350°C for 60 min under He (inert) gas conditions followed by NH3 adsorption and desorption procedures. Thermogravimetric analysis (TGA) was carried out with a LINSEIS-L70/2171 apparatus, the temperature was increased at a rate of 10°C/min at 30°C to 1000°C with nitrogen flow. Surface Area Analyzer (SAA) based on Brunauer-Emmet-Teller (BET) method of Micromeritics TriStar II 3020 manufactured with adsorptive N_2 analysis and 10s equilibration interval, sample mass 0.35 g, cold free space 32.81 cm³, sample density 1 g/cm³, Barret-Joyner-Halenda (BJH) method to identify specific surface area and porosity.

2.3 Catalyst Analysis

In this study, a total of all catalysts namely bentonite, Al/bentonite, Ni/bentonite, Mn/bentonite, Al-Mn/bentonite, and Al-Ni/bentonite were applied in the catalytic conversion process of ethanol to biogasoline using a batch-scale autoclave reactor. The catalyst was used at 5% (1:20 g/mL) of the feed, which was ethanol. A total of 0.5 g of the catalyst was weighed and added to the reactor along with 10 mL of ethanol. The reactor is supplied with H2 gas and then purged, repeated 3 times, and H₂ gas is flows back as much as 1 atm for the reaction process. The temperature was set at 150°C for 3 hours with a stirring speed of 200 rpm. The reaction product was filtered using Whatman paper, and the resulting liquid was prepared for analysis. The product was analyzed using Chromatography-Flame Ionization Detector (GC-FID) type Agilent 113-2032 Carbowax/20M column (30 m x 320 µm, 25 µm) and FID detector.

3. Results and Discussion

3.1 Measurement with X-Ray Diffraction (XRD)

X-ray diffraction (XRD) was used to confirm the structural changes in bentonite before and after pillarization with metal oxide pillars. After pillarization, the XRD measurement determined the basal space distance (d₀₀₁) between bentonite interlayers. The standard pattern COD Card Number 96-901-0958 shows diffraction peaks at $2\theta = 19.83^{\circ}$, 26.51° , 34.81° , 54.05° , and 61.94° , indicating bentonite structure of the montmorillonite type. Basal spacing sizes (d₀₀₁) are typically measured at an angle of $2\theta < 100$ to determine if pillarization occurred. The intercalation or pillarization process caused a shift in the d₀₀₁ diffraction peak toward a lower angle, indicating an increase in basal spacing. Fig. 1 displays the XRD results of

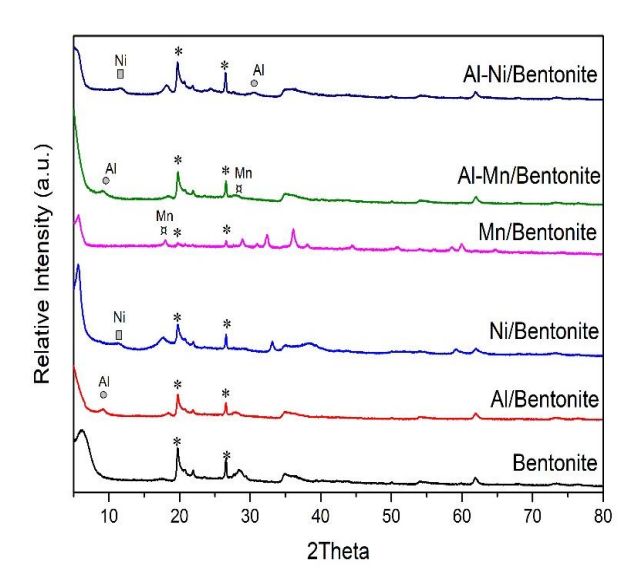


Fig. 1 X-ray diffraction (XRD) diffractogram of various catalyst and the support

pillared bentonite treated with metal oxide Aluminium, Manganese, and Nickel. Fig. 1 shows that pillarization with Al polycations shifts the diffraction peak from 6.35° to 5.01° (Al/Bentonite), 5.66° (Ni/Bentonite), 5.71° (Mn/Bentonite), 5.1° (Al-Mn/Bentonite), and 5.01 (Al-Ni/Bentonite). The change in the d₀₀₁ diffraction peak indicates an increase in basal spacing. This occurs due to the exchange of cations in the bentonite interlayer with Al, Mn, and Ni polycations. The surface area measurement in Table 2 showed substantial results. However, the surface area measurement results in Table 2 indicated a large increase during the pillarization process in bentonite layers with Al, Mn, and Ni metals.

The pillarization of bentonite with Al, Mn, and Ni metal oxides doesn't change the structure of montmorillonite. Montmorillonite's diffraction peaks persist even after pillarization. The distinctive diffraction peaks can be observed in the wide-angle diffraction pattern at $2\theta=10^{\circ}$ -80°. Fig. 1 shows the XRD data for pillared Al/Bentonite, Ni/Bentonite. Mn/Bentonite, Al-Mn/Bentonite, Al-Ni/Bentonite catalysts. The intensity of diffraction peaks of Mn/Bentonite decreases, this suggests that manganese, as a pillar metal, interacts with the crystalline structure of bentonite, forming of manganese metal oxide. The Characteristic structure of MnO₂ is represented by diffraction peaks at $2\theta=32.37^{\circ}$ and 36.13° , as seen in the standard pattern COD Card Number 96-101-1263. All samples show different peaks because each metal has different characteristics.

The results of XRD measurements for Ni/bentonite with Al-Ni/bentonite show a change in difraction peaks, this is because Al metal influences the structure of bentonite. Aluminium crystal planes show a diffraction peak at $2\theta=19.75^{\circ}$, and peaks at $2\theta=26.57^{\circ}$, 28.03° , and 35.07° , as per the standard pattern COD Card Number 96-900-9667. Fig. 1 shows a new diffraction peak at $2\theta=9.14^{\circ}$ for Al/Bentonite, 11.25° for Ni/Bentonite, 32.37° for Mn/Bentonite, 9.10° for Al-Mn/Bentonite, and 11.55° for Al-Ni/bentonite, which corresponds to the aluminium peak. Polycation Al metal pillarization resulted in new diffraction peaks at $2\theta=9.14^{\circ}$ and 19.75° , indicating Al_2O_3 . The XRD data indicate a successful preparation of pillarization bentonite with Al, Ni and Mn metal oxides.

Diffraction peaks at $2\theta=19.8^{\circ}$, 34.9° , and 61.9° correspond to montmorillonite (COD Card Number 96-900-5020), while diffraction peaks at $2\theta=21.78^{\circ}$, 26.62° , and 36.51° correspond to SiO₂ (COD Card Number 96-901-0145), indicating a typical bentonite support (Jiang et al., 2016). In Ni/bentonite, diffraction peaks of NiO were identified at $2\theta=5.66^{\circ}$, 42.65° , 61.98° and 76.54° , corresponding to the (111), (200), (220), (311), and (222) planes of the cubic phase NiO, respectively. The diffraction peak intensity of NiO in bentonite appeared well-defined, this is because NiO particles had excellent dispersity and the size of metallic nickel particles was reduced (Li et al., 2015; Lu et al., 2015).

3.2 Measurement with X-Ray Fluorescence (XRF)

X-ray fluorescence (XRF) characterization was used to measure the distribution of components in bentonite before and after pillarization. The XRF results for the produced catalysts are shown in Table 1. The XRF analysis of bentonite reveals the presence of elements such as Al³+, Si²+, Fe³+, and Ca²+, but no Na⁺. The study confirmed the use of Ca-Montmorillonite bentonite based on its elemental composition. After pillarization, the Mn and Ni components increased, but other elements in the initial bentonite (Al, Si, Fe, and Ca) decreased. However, the number of element compounds in bentonite dropped following pillarization. The pillarization process affects the interlayer area of the bentonite layers (Montmorillonite) and

 Table 1

 Chemical composition of various catalyst and the support

Samples	Elements (%)						
	SiO ₂	Al_2O_3	Fe_2O_3	MgO	CaO	MnO	NiO
Bentonite	62.57	23.03	5.01	3.64	1.55	-	-
Al/Bentonite	58.26	30.66	5.16	3.45	0.19	-	-
Ni/Bentonite	39.79	14.97	2.95	1.89	0.74	-	37.50
Mn/Bentonite	32.81	10.89	3.07	1.66	0.74	48.65	-
Al-Mn/Bentonite	56.90	31.40	5.10	3.20	0.20	0.70	-
Al-Ni/Bentonite	51.30	36.80	3.90	2.90	0.20	-	2.40

does not change the strength of their structure. Mn/bentonite has a large Mn content, namely 48.65%. This shows that the process of inserting pillar metal into bentonite has been successful. Similarly, the Ni/Bentonite sample has Ni content of 37.50%, this is confirmed by the XRD measurement results. The Al-Mn/bentonite bimetallic sample contains a lower Mn content compared to Mn/Bentonite, at 0.70%. This is due to the large number of Al metal molecules entering the bentonite pores. Therefore, the Mn metal to remain on the surface of the bentonite. Likewise, Al-Ni/Bentonite has a Ni content of 2.40%, which is smaller than that of Ni/Bentonite sample.

The Al-Ni/Bentonite and Al-Mn/Bentonite catalysts show an increase in the composition of Al_2O_3 oxide, though the increase is not very significant. The Al-Ni/Bentonite catalyst has a greater increase in Al_2O_3 composition compared to Al-Mn/Bentonite. This is evident from the greater decrease in bentonite oxide, indicating that the cation exchange process occurs more extensively in Al-Ni/Bentonite than in the Al-Mn/Bentonite catalyst. The increase in NiO oxide was 2.40% greater than MnO, due to diffusion barriers with the number of intercalated Al molecules. The ion charge and diameter of the Ni and Mn metal molecules also influenced it.

In the Al-Ni/Bentonite catalyst, there is a decrease in SiO_2 and Fe_2O_3 oxides, and other bentonite oxides, which causes a greater increase in the pillar metal. This shows that cation exchange occurs almost completely. NiO oxide has a percentage of 37.5% along with an increase in MnO oxide of 48.65%. This is also confirmed in the XRD data in Fig. 1, which shows a decrease in the intensity of the typical bentonite peak, accompanied by the growth of new peaks for NiO and MnO, which dominate the spectrum.

3.3 Measurement with Surface Area Analyzer (SAA)

The purpose of characterizing the prepared catalysts is to determine the success or failure of the pillarization method. The Brunauer-Emmett-Teller (BET) method determines the surface area, pore volume, and pore size of pillared bentonite using nitrogen gas adsorption and desorption (N₂). Table 2 displays the adsorption results for nitrogen gas using the produced catalysts. Table 2 demonstrates that pillared bentonite with aluminium, nickel, and manganese polycations significantly increased surface area, pore volume, and pore size. Raw

Table 2Physicochemical properties of various catalyst and the support

-	Surface	Pore Volume	Pore Size	
Catalyst	Area (m²/g)	(cm3/g)	(Å)	
Bentonite	25.15	0.09	13.87	
Al/Bentonite	187.84	0.16	33.21	
Ni/Bentonite	74.97	0.15	79.29	
Mn/Bentonite	39.27	0.21	210.12	
Al-Mn/Bentonite	151.61	0.13	35.21	
Al-Ni/Bentonite	76.07	0.08	44.60	

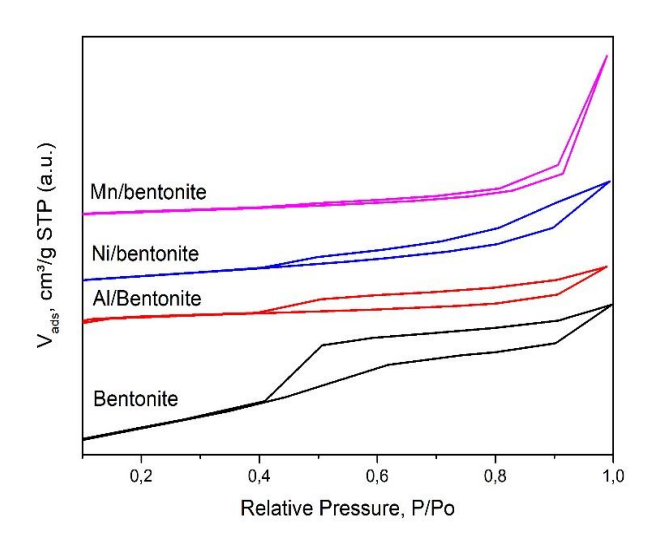


Fig. 2 N2 adsorption-desorption isotherm of Al, Ni, Mn and the support

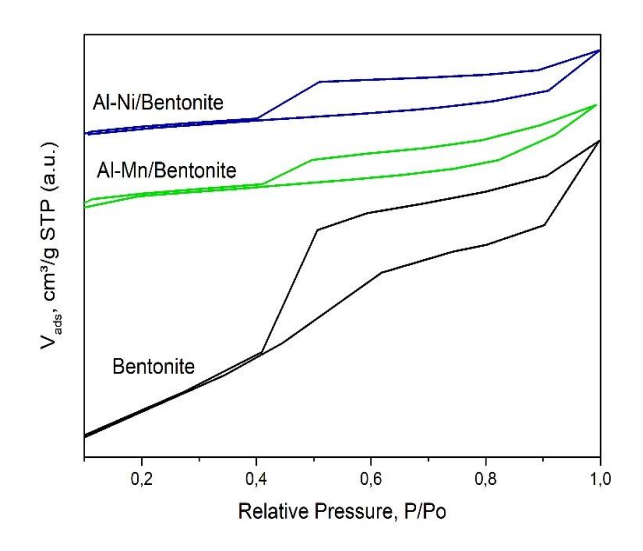


Fig. 3 N2 adsorption-desorption isotherm of Al-Mn, Al-Ni, and the support

bentonite has a surface area of 25.15 m²/g, a pore volume of 0.09 cm³/g, and a pore size of 13.87 Å. After pillarization with metal oxides Al, Ni, and Mn, the surface area, pore volume, and pore size rise to 187.84 m²/g, 0.16 cm³/g, and 33.21 Å for Al/Bentonite, and 74.97 m²/g, 0.15 cm³/g, 79.29 Å for Ni/Bentonite catalysts, respectively. The increased surface area on Al/Benonite and Ni/Bentonite catalysts may be attributed to the strong bonding of Al³+ or Ni²+ cations in the bentonite interlayer found that adding aluminium oxide and nickel oxide

Table 3Acidity of various catalyst and the support

yyyy					
Catalyst	Acidity (mmole/g)				
Bentonite	0.29				
Al/Bentonite	2.27				
Ni/Bentonite	2.26				
Mn/Bentonite	1.22				
Al-Mn/Bentonite	2.31				
Al-Ni/Bentonite	2.33				

pillars to the interlayer space of bentonite resulted in a considerable increase in surface area and pore volume.

The stages of the pillarization method for bentonite pillars produced interesting outcomes. Pillared bentonite exhibited a significant increase in surface area, pore volume, and pore size, particularly for Al/Bentonite and Al-Mn/Bentonite catalysts. Aluminium metal may contribute to the fragmentation of particles into smaller smaller, more homogenous components. The pillarization process substantially enhances the surface area of pillared bentonite compared to raw bentonite. Table 2 demonstrates that the Al-Mn/Bentonite catalyst has a greater surface area (151.61 m²/g) when using bimetallic pillarization.

Fig. 2 displays the adsorption-desorption isotherm curve for raw bentonite. Sing et al. (2008) classified pore size according to IUPAC into three categories: micropores (< 2 nm), mesopores (2-50 nm), and macropores (> 50 nm) (Sing et al., 2008). Raw bentonite has a mesoporous structure with a pore size of 13.86 nm. The adsorption-desorption isotherm graph of raw bentonite in Fig. 2 aligns by Thommes et al. (2015), identifying bentonite as a type IV isotherm with mesoporous pores. The graph is classified as an H3 hysteresis loop, similar to those typically observed in clay (bentonite). Fig. 3 shows the adsorptiondesorption isotherm graph of the produced catalyst. In Fig. 3, the Al-Ni/Bentonite and Al-Mn/Bentonite catalysts show type IV isothermal graphs for adsorption and desorption. Both catalysts display an H4 hysteresis loop pattern, which is often associated with the predominance of micropores. The surface area of a catalyst is a crucial factor in determining its activity. A large surface area implies greater interaction and more active metal sites between oleic acid and the Al-Ni/Bentonite and Al-Mn/Bentonite catalysts, leading to increased catalytic activity.

3.4 Measurement with Temperature Programmed Desorption-Ammonia (NH₃-TPD)

The acid strength measurement was performed using the NH_3 -TPD equipment to determine the amount of NH_3 gas adsorption on the surface catalyst. The total amount of NH_3 gas adsorption indicates the catalyst's acid strength (acidity) (Supeno & Siburian, 2018). Table 3 displays the acidity measurement results for the catalysts produced using NH_3 -TPD. Table 3 demonstrates that acidity properties of pillared bentonite increased dramatically compared to raw bentonite. The process of cation exchange with Al, Mn, Ni, Al-Mn, and Al-Ni pillar metal oxides occurs in the interlayer bentonite.

The successful exchange of cations with Al, Mn, Ni, Al-Mn, and Al-Ni pillar metal oxides in interlayer bentonite has significantly increased acidity (Agustian *et al.*, 2021). Several studies show that during pillarization, the exchange of cations in the bentonite interlayer with Al³⁺, Mn²⁺, and Ni²⁺ cations of Al, Mn, and Ni metal oxides results in the creation of numerous acid sites (Alzamel, 2022). The pillarization also causes an extension of the interlayer on the pillared bentonite, increasing the number of protons that serve as acid sites (Darmawan et al., 2019). Table

3 further shows that the pillarization method for Al/Bentonite, Mn/Bentonite, and Ni/Bentonite catalysts is more acidic than raw bentonite. The pillarization procedure quickly changes the pillaring metal agent in the interlayer bentonite.

The Temperature Programmed Desorption-NH₃ (NH₃-TPD) device is used to analyze acid-strength catalysts via chemisorption, measuring the amount of NH3 gas adsorbed and desorbed. The amount of NH₃ gas absorbed is proportional to the acidity of the catalyst (Peng et al., 2014). Table 3 shows the results of the NH3-TPD study on the produced catalysts. It shows that the total acidity of Al/Bentonite, Mn/bentonite, Ni/Bentonite, Al-Mn, and Al-Ni/bentonite is higher than that of raw bentonite. This is due to the successful cation exchange process in the bentonite interlayers with Al, Mn, and Ni pillar metals, which increased the acidity strength of the bentonite supported by these metals. This enhancement is supported by the greater oxidation state and charge of Al, Mn, and Ni metals, which allow them to exchange with buffering cations (Johansson et al., 2009). It is also influenced by the silanol layer structure, where the supporting metal's oxide is completely exchanged for Al, Mn, and Ni ions. Al ions on the support combine with Al-Si-OH group bonding to generate medium to strong acid sites (Parangi & Mishra, 2020).

Furthermore, this study shows that pillaring Al, Mn, and Ni in bentonite can greatly increase the acidity of the modified bentonite (Salerno *et al.*, 2004). The acidity levels of Al/Bentonite, Ni/Bentonite, and Mn/Bentonite increase after pillarization with these metals, with a notable increase observed in Mn/Bentonite (Table 3). This finding is supported by XRD data (Fig. 1), which indicate the absence of distinctive MnO peaks, suggesting that Mn metal is evenly distributed on the bentonite surface, thereby enhancing acidity (He, Y. et al., 2018). Similar to Mo, the pillarization of Ni metal into the catalyst further strengthens its acid properties. The results (Table 3) show that when Al/Bentonite is pillared with Ni to form Al-Ni/Bentonite, acidity increases, although not significantly.

In contrast, introducing Mn to bentonite results in a slight decrease in acid strength, possibly due to Mn metal covering the catalyst's acidic sites (Sun Kou et al., 2000). Additional evidence supporting the well-dispersed Al and Ni metals contributing to higher acid strength is the decrease in specific surface area (Table 2). Catalysts with Ni-based pillars exhibit higher total acidity than Mn-based catalysts because the positive charge of Ni²+ ions is greater than that of Mn²+ ions. (Binitha & Sugunan, 2006).

3.5 Measurement with Thermogravimetric Analysis (TGA)

The relative mass decrease of bentonite and modified bentonite catalysts increases as the heating temperature rises. The percentage change in total mass, based on TGA analysis of bentonite, Al/Bentonite, Ni/Bentonite, and Mn/Bentonite catalysts was 4.89, 12.63, 16.06, and 34.36% respectively. The first stage of mass change corresponds to the release of water molecules (dehydration), which are physically bound to the surface of the catalyst structure. Some catalysts, such as the Mn-PILC catalyst, begin to undergo mass change at a relatively lower temperature than others, specifically at 260°C, making the catalyst unstable to heat from that temperature onward.

The decomposition process of catalyst materials as a function of temperature results in a decrease in material weight when heated from 400°C to 700°C. Based on Fig. 5, the formation of the TGA curve for bentonite shows the first mass decrease starting at a temperature of 49.71°C. The Al-Ni/Bentonite, and Al-Mn/Bentonite catalysts exhibit a significant decrease in mass on the TGA curve in three stages,

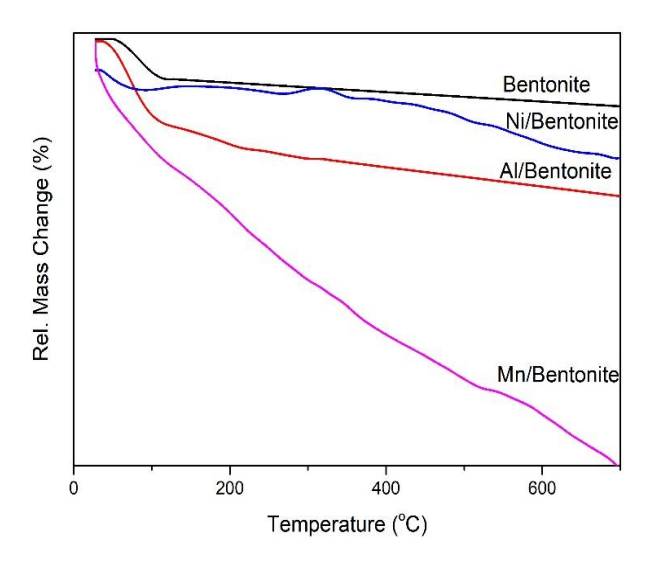


Fig. 4 TGA curve of Al, Ni, Mn, and the support

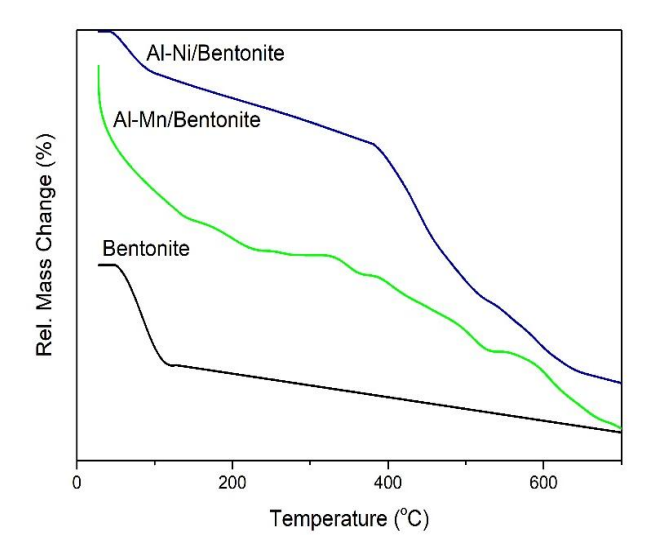


Fig. 5 TGA curve of Al-Mn, Al-Ni, and the support

indicating the maximum temperature the catalyst material can withstand before total degradation due to heating. Parangi *et al.* (2020) reported that the reaction is considered complete when the exothermic peak temperature is reached, as shown in Fig. 4. The Al and Ni/Bentonite catalysts demonstrate higher thermal stability, which is influenced by the presence of Al and Ni metals, both of which have higher melting points than Mn metal. The addition of mixed metal oxides Al₂O₃, NiO, and MnO enhances the physical properties of the bentonite structure, thereby increasing the thermal stability of the catalyst material. Below is the data from the TGA analysis based on three stages of catalyst mass reduction.

The relative mass decrease in bentonite catalyst and bimetallic pillared bentonite increases as the heating temperature rises. The total mass change, based on TGA analysis of bentonite, Al-Ni/Bentonite, and Al-Mn/Bentonite catalysts, was 4.89%, 10.34%, and 10.63% respectively. A greater total mass change indicates a higher storage capacity for the reaction process. In the first stage, the mass change signifies the dehydration process on the surface of the catalyst structure. The Al-Mn/PILC catalyst begins to exhibit mass change at 35°C, making the catalyst unstable at that temperature. Meanwhile, the Ni-Mn/PILC catalyst shows the highest temperature value, with the initial mass change occurring in the

second stage at the temperature of 289°C. This indicates that the catalyst has very low water content, as the two metals embedded on the surface and within the interlayer significantly enhance the material's durability.

The second stage of mass change occurs within the temperature range of 92°C-700°C. Rinaldi et al. (2023) indicated that dehydroxylation and structural changes occur in bentonite cation oligomers. The increase resulting in temperature, which refers to the process of formation of metal oxide pillarization, which results in structural changes. In the third stage, the sample is inert, the mass reduction is measured slightly. However, it was indicated that the maximum dehydroxylation process occurs in the metal oxide pillar structure, which results in damage to the alumina-silica structure of bentonite.

3.6 Measurement with Fourier Transform Infrared Spectroscopy (FTIR)

The acidity levels in PILC catalysts due to pillarization were qualitatively determined using infrared spectroscopy (FTIR) in the wave umber range of 4000-400 cm⁻¹. The primary requirement for determining absorption potential catalytic utilization is identifying the acid sites on the surface of the material, as indicated by the presence of Lewis and Bronsted acid sites (Rodiansono et al., 2007). The presence of acid sites on the surface of bentonite and pillared bentonite determines their role and activity in catalysis, with Bronsted and Lewis acid sites, which are the most common. The Brønsted acid site can release H⁺ions, while Lewis acid sites can accept electron pairs. The acidity of materials can be evaluated using the absorption method, with pyridine as the adsorbate base (Wang et al., 2017). Pyridine molecules are protonated and adsorbed at specific infrared wave number: 1620 cm-1 for Bronsted acid sites and 1440 cm⁻¹ for Lewis acid sites. The interaction of pyridine molecules with Bronsted and Lewis acid sites is represented in the wave number range of 1490-1493 cm-1 (Bahranowski et al.,

The PILC shows a peak at a wave number of 1483 cm⁻¹, indicating that pyridine vapor interacts with Lewis acid sites. After pillarization, acid strength increased, as evidenced by the larger peak areas in Al/Bentonite, Ni/Bentonite, and Mn/Bentonite. Al/bentonite exhibits two peaks: 1483 cm-1 for Lewis acid sites and 1632 cm⁻¹ for Brønsted acid sites, similar to Ni/Bentonite and Mn/Bentonite. Al-Mn/Bentonite contains two peaks at 1631 cm⁻¹ for the Brønsted acid sites and 1438 cm⁻¹ for the Lewis acid sites. These data indicate that pillared

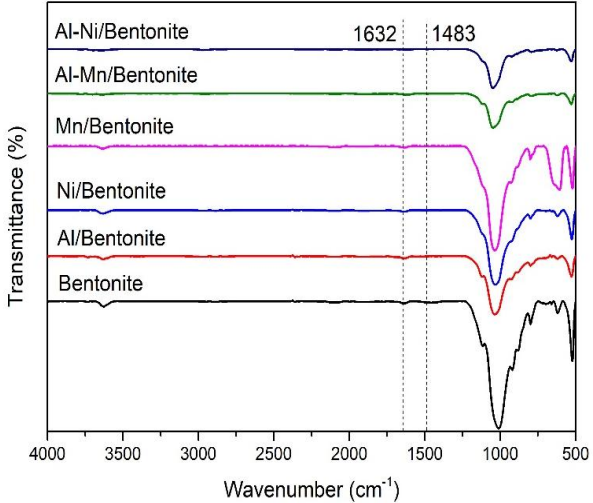


Fig. 6 FTIR spectra of various catalyst and the support

Al/Benonite, Ni/Bentonite, and Mn/Bentonite have higher acid strength than raw bentonite (Daroughegi *et al.*, 2019).

Fig. 6 shows the FTIR analysis results for all the catalyst samples, with each catalyst producing distinct types of acid sites. Bentonite exhibits six characteristic absorption in the FTIR spectrum, detected at wavenumbers 522 cm⁻¹, 619 cm⁻¹, 797 cm⁻¹, 1011 cm⁻¹, 1634 cm⁻¹, and 3627 cm⁻¹. The absorption peak at wave number 522 cm⁻¹ corresponds to the bending vibration of Si-O-Si in the aluminosilicate bentonite framework, while the peak at 1011 cm⁻¹ indicates the stretching vibration of Si-O-Si. These bending and stretching vibrations confirm the presence of an aluminosilicate framework in the catalyst. Additionally, the bending vibration of Si-O-Al in bentonite occurs at the 522 cm⁻¹ absorption peak. The absorption at 1632 cm⁻¹ corresponds to the -OH bending vibration of water molecules adsorbed in the bentonite interlayer. Furthermore, the absorption peak at 3627 cm⁻¹ confirms the presence of H-O-H stretching vibrations, indicating the formation of hydrogen bonds with water molecules.

3.7. Measurement with Gas Chromatography-Flame Ionization Detector (GC-FID)

The performance of the prepared catalyst was analyzed using GC-FID (Gas Chromatography-Flame Iniozed) based on the conversion value (%), and biogasoline selectivity (%). The percent conversion values are shown in Fig. 7. The analysis of compound components was conducted qualitatively by comparing the retention time and area with Pertalite gasoline standards. Ethanol was successfully converted with varying yield levels. This catalytic process aims to demonstrate the effect of bentonite modification as a catalyst through the pillarization method in converting ethanol into biogasoline products.

The Bentonite catalyst has a conversion value of 0.03%. In comparison, the conversion value significantly increases with the pillared bentonite catalysts. Al/Bentonite exhibits the highest conversion value among the pillared bentonite catalysts, at 68.64%. This is due to the superior physicochemical properties of the catalyst, such as interlayer spacing, surface area, and acidity (Huang et al., 2022). These differences are typically attributed to variations in active site availability, reaction kinetics, and stability under process conditions. Al/Bentonite catalysts are well-optimized for hydrogenation and related reactions, benefiting from high surface area, strong metal-support interactions, and controlled selectivity (Hamouda

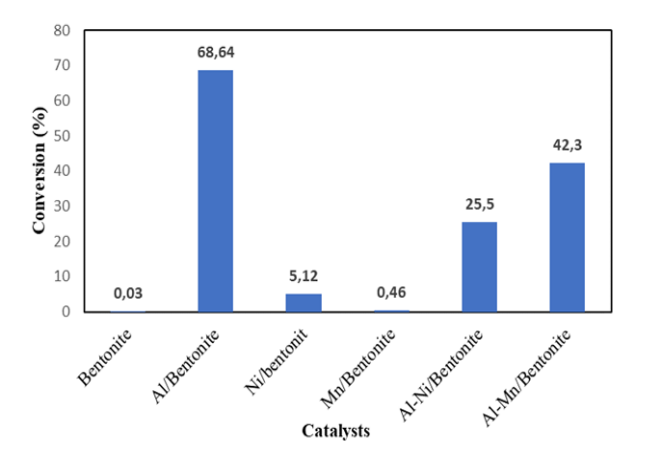


Fig. 7 The conversion percentage of liquid products from ETG reaction

et al., 2021). The catalytic activity of Ni and Mn, in particular, is highly dependent on their oxidation states. Ensuring proper reduction and activation conditions can significantly impact efficiency. Reaction conditions, including temperature, pressure, and reactant ratios, also play a crucial role in optimizing bimetallic/alloy catalysts, which may not always be ideal for performance. Mn/Bentonite has a conversion value of 0.46%, which is an improvement compared to bentonite but remains low compared to other pillared bentonites. However, Mn/Bentonite has a higher thermal stability value than other catalysts. Al-Mn/Bentonite achieved a conversion value of 42.3%, which is higher than that of bentonite and Mn/Bentonite, but lower than that of Al/Bentonite.

Mixed metal-pillared bentonite catalysts have high potential because the combination of two different metal properties can form oxide-pillared bentonite with more specific catalytic and adsorption properties, effectively compensating for the shortcomings of each metal (Widjaya et al., 2021). As reported in previous studies, Widjaya et al. (2021) found that Sn-Cr-PILC and Fe-Cr-PILC catalysts produced higher conversion values compared to their single metal counterparts. However, pillarization using Mn metal reduced the physicochemical properties of bentonite, making catalysis less effective. Key parameters such as surface area and acidity showed a decline. Gandia et al. (1998) reported that the presence of Mn, when combined with the pilarization method, could cause a significant decrease in the textural properties of the final material.

Al-Ni Bentonite provides high selectivity, but with low conversion in many catalytic reactions (Suseno *et al.*, 2019). This is due to several main factors: Acidic and Basic Properties, Al-Ni/Bentonite has weakly acidic active sites, which can increase selectivity to certain products but limit the extent of reactant conversion. The porous structure of bentonite affects the diffusion of reactants and products (Galeano *et al.*, 2014). If the pores are narrow or not optimal, reactants may have difficulty reaching the active sites, reducing conversion. Nickel is often used in hydrogenation catalysts and other reactions. However, in bentonite-based systems, Ni interactions with the bentonite surface can reduce the availability of Ni active sites, thereby reducing reaction efficiency (Aid et al., 2017).

Al-Ni/Bentonite is more commonly used for selective reactions such as partial hydrogenation or deoxygenation, where the goal is to produce specific products while minimizing side reactions (Cardona et al., 2021). However, if high conversion is desired, it may be necessary to combine it with other catalysts or modify the bentonite to increase its activity (Wen et al., 2019). Al-Ni catalyst affects the optimal carbon chain cracking process to produce specific n-heptane products. So, the n-heptane content value dominates the selectivity value in gasoline (Rafiani et al., 2020). Meanwhile, because the conversion value is dominated by the cracking results of the single metal Al catalyst, the conversion value of Al-Ni is low. Al alone can achieve a very high conversion value due to its exceptionally large specific surface area, which increases the capacity for the conversion reaction to occur on a larger scale. (Furimsky et al., 2000).

Component analysis of biogasoline compounds formed from the catalytic conversion of ethanol determined the selectivity of each compound, as presented in Table 4. Biogasoline compounds resulting from the catalytic conversion of ethanol produce products with carbon chains ranging from C_6 - C_{12} , in the form of paraffin and aromatic compounds. Ethanol (C_2H_5OH) undergoes dehydration, alkylation, and cracking, leading to the breaking and recombining of carbon chains, thereby extending the carbon chain length from C_6 to C_{12} (Widjaya et al., 2012). The conversion of ethanol to gasoline (ETG) using bentonite and modified bentonite catalysts results in the formation of

several key compounds found in gasoline. The differences in selectivity are determined by the area at a specific retention time, as detected by the GC-FID detector. The compounds in the samples were identified by comparing them with the standard compound in Pertalite gasoline. If the retention time of the sample peak closely matches the retention time of a standard peak, the sample is considered to contain similar compound components (Sudarma & Parwata, 2017). The transformation of ethanol (C₂) into hydrocarbons in the C₆-C₁₂ range is evident. The conversion results show that the Al-Ni/Bentonite catalyst has the highest biogasoline selectivity at 58.09%, with a higher n-heptane (C_7H_{16}) content (58.03%) than other catalysts. Al/Bentonite catalyst exhibits a biogasoline selectivity of 51.697%, which is slightly lower. However, the conversion results and biogasoline selectivity for all catalysts show a linear relationship.

4. Conclusion

Based on the results of this research, it can be concluded that the synthesis of a modified bentonite catalyst enhances physicochemical characteristics, including basal spacing, specific surface area, thermal stability, and acidity. The modified bentonite catalyst exhibits improved physicochemical properties that positively influence the conversion process. These enhanced physicochemical properties contribute to the catalytic conversion of ethanol to biogasoline. The Al/Bentonite catalyst achieved the highest conversion rate of 68.64% in the ethanol-to-gasoline reaction, while the Al-Ni/Bentonite catalyst demonstrated has the highest selectivity, at 58.09%.

Acknowledgments

The authors would like to acknowledge financial support from the BRIN through Scheme of Riset & Inovasi untuk Indonesia Maju (RIIM) and the funding scheme of the nanotechnology and materials research organization BRIN. The Indonesian Endowment Fund for Education (LPDP) also partly funded this study.

References

- Agustian, E., Rachmawati, A., Purba, N. D. E., Rinaldi, N., & Juwono, A. L. (2021). Effect of ultrasonic treatment on the preparation of zirconia pillared bentonite as a catalyst. *Journal of Physics: Conference Series, 1951*(1), 012017. https://doi.org/10.1088/1742-6596/1951/1/012017
- Aid, A., Andrei, R. D., Amokrane, S., Cammarano, C., Nibou, D., & Hulea, V. (2017). Ni-exchanged cationic clays as novel heterogeneous catalysts for selective ethylene oligomerization. Applied Clay Science, 146, 432–438. https://doi.org/10.1016/j.clay.2017.06.034
- Alzamel, M. (2022). Swelling ability and behaviour of bentonite-based materials for deep repository engineered barrier systems: Influence of physical, chemical and thermal factors. *Journal of Rock Mechanics and Geotechnical Engineering*.
- Bahranowski, K., Włodarczyk, W., Wisła-Walsh, E., Gaweł, A., Matusik, J., Klimek, A., Gil, B., Michalik-Zym, A., Dula, R., Socha, R. P., & Serwicka, E. M. (2015). [Ti,Zr]-pillared montmorillonite A new quality with respect to Ti- and Zr-pillared clays. *Microporous and Mesoporous Materials*, 202, 155–164. https://doi.org/10.1016/j.micromeso.2014.09.055
- Binitha, N. N., & Sugunan, S. (2006). Preparation, characterization and catalytic activity of titania pillared montmorillonite clays. *Microporous and Mesoporous Materials*, *93*(1–3), 82–89. https://doi.org/10.1016/j.micromeso.2006.02.005
- Cardona, Y., Korili, S. A., & Gil, A. (2021). Understanding the formation of Al13 and Al30 polycations to the development of microporous

- materials based on Al13-and Al30-PILC montmorillonites: a review. Applied Clay Science, 203, 105996. https://doi.org/10.1016/j.clay.2021.105996
- Darmawan, A., Fuad, K., & Azmiyawati, C. (2019). Synthesis of chromium pillared clay for adsorption of methylene blue. *IOP Conference Series: Materials Science and Engineering*, 509, 012003. https://doi.org/10.1088/1757899X/509/1/012003
- Daroughegi Mofrad, B., Rezaei, M., & Hayati-Ashtiani, M. (2019). Preparation and characterization of Ni catalysts supported on pillared nanoporous bentonite powders for dry reforming reaction. International Journal of Hydrogen Energy, 44(50), 27429–27444. https://doi.org/10.1016/j.ijhydene.2019.08.194
- Fatimah, I., Narsito, N., & Wijaya, K. (2011). Effect of Aluminium Content in Aluminium Pillared Montmorillonite on Its Surface Acidity Properties. *ITB Journal of Sciences*, 43(2), 123–138. https://doi.org/10.5614/itbj.sci.2011.43.2.5
- Furimsky, E. (2000). Catalytic hydrodeoxygenation. Applied Catalysis A: General, 199(2), 147–190. https://doi.org/10.1016/S0926-860X(99)00555-4
- Gandía, L. M., Vicente, M. A., Oelker, P., Grange, P., & Gil, A. (1998).
 Preparation and characterization of manganese- and samarium-manganese-alumina pillared montmorillonites. *Reaction Kinetics and Catalysis Letters*, 64(1), 145–151.
 https://doi.org/10.1007/BF02475382
- Goldemberg, J. (2007). Ethanol for a Sustainable Energy Future. Science, 315(5813), 808–810. https://doi.org/10.1126/science.1137013
- Galeano, L.-A., Vicente, M. Á., & Gil, A. (2014). Catalytic Degradation of Organic Pollutants in Aqueous Streams by Mixed Al/M-Pillared Clays (M = Fe, Cu, Mn). Catalysis Reviews, 56(3), 239–287. https://doi.org/10.1080/01614940.2014.904182
- Hamouda, A. S., Acharjee, P., Abdelrahman, A., Radwan, A. M., Zaki, A.
 H., Farghali, A., Goel, A. (2021). Catalytic thermochemical cracking of polyethylene over nanocomposite bentonite clay. IOP Conference Series: Materials Science and 104 Engineering, 1046(1), 012022. https://doi.org/10.1088/1757-899X/1046/1/012022
- He, Y., Jiang, D. B., Chen, J., Jiang, D. Y., & Zhang, Y. X. (2018). Synthesis of MnO2 nanosheets on montmorillonite for oxidative degradation and adsorption of methylene blue. Journal of Colloid and Interface Science, 510, 207–220. https://doi.org/10.1016/j.jcis.2017.09.066
- Huang, H., Fang, T., Liu, H., Zhou, H., Chen, D., Jia, W., Zhu, Z. (2022).

 Ethanol-to-hydrocarbons reaction over HZSM-5: Enhanced ethanol/ethylene into C3+ hydrocarbons conversion by pristine external Brönsted acid sites. Microporous and Mesoporous Materials, 335, 111824. https://doi.org/10.1016/j.micromeso.2022.111824
- Jiang, Y., Li, X., Qin, Z., & Ji, H. (2016). Preparation of Ni/bentonite catalyst and its applications in the catalytic hydrogenation of nitrobenzene to aniline. *Chinese Journal of Chemical Engineering*, 24(9), 1195–1200. https://doi.org/10.1016/j.cjche.2016.04.030
- Johansson, R., Hruby, S. L., Rass-Hansen, J., & Christensen, C. H. (2009). The Hydrocarbon Pool in Ethanol-to-Gasoline over HZSM-5 Catalysts. Catalysis Letters, 127(1-2), 1-6. https://doi.org/10.1007/s10562-008-9711-2
- Kumar Dutta, D., Jyoti Borah, B., & Pollov Sarmah, P. (2015). Recent Advances in Metal Nanoparticles Stabilization into Nanopores of Montmorillonite and Their Catalytic Applications for Fine Chemicals Synthesis. *Catalysis Reviews*, 57(3), 257–305. https://doi.org/10.1080/01614940.2014.1003504
- Li, D., Zeng, L., Li, X., Wang, X., Ma, H., Assabumrungrat, S., & Gong, J. (2015). Ceria-promoted Ni/SBA-15 catalysts for ethanol steam reforming with enhanced activity and resistance to deactivation. Applied Catalysis B: Environmental, 176–177, 532–541. https://doi.org/10.1016/j.apcatb.2015.04.020
- Lu, X., Gu, F., Liu, Q., Gao, J., Liu, Y., Li, H., Jia, L., Xu, G., Zhong, Z., & Su, F. (2015). VOx promoted Ni catalysts supported on the modified bentonite for CO and CO2 methanation. *Fuel Processing Technology*, 135, 34–46. https://doi.org/10.1016/j.fuproc.2014.10.009
- Okoye, I. P., & . C. O. (2011). Synthesis and Characterization of Titanium Pillared Bentonite Clay Mineral. *Research Journal of Applied Sciences*, 6(7), 443–446. https://doi.org/10.3923/rjasci.2011.443.446

- Parangi, T., & Mishra, M. K. (2020). Solid Acid Catalysts for Biodiesel Production. *Comments on Inorganic Chemistry*, 40(4), 176–216. https://doi.org/10.1080/02603594.2020.1755273
- Peng, S.-Y., Xu, Z.-N., Chen, Q.-S., Wang, Z.-Q., Chen, Y., Lv, D.-M., Lu, G., & Guo, G.-C. (2014). MgO: An excellent catalyst support for CO oxidative coupling to dimethyl oxalate. *Catalysis Science & Technology*, 4(7), 1925–1930. https://doi.org/10.1039/C4CY00245H
- Rafiani, A., Aulia, F., Dwiatmoko, A. A., Rinaldi, N., Nurhasni, & Widjaya, R. R. (2020). Studies on Nickel-based Bimetallic Catalysts for the Hydrodeoxygenation of Stearic Acid. IOP Conference Series: Materials Science and Engineering, 722(1), 012001. https://doi.org/10.1088/1757-899X/722/1/012001
- Ramadhaniati, D., Saridewi, N., Dwiatmoko, A. A., Rinaldi, N., Ramdani, D., Putri, A. M. H., Widjaya R. R. (2023). Aluminium and zirconium pillared bentonite for ethanol to gasoline conversion process. *AIP Conf. Proc.* 2902, 030001. https://doi.org/10.1063/5.0173147
- Rinaldi, N., Purba, N. D. E., Kristiani, A., Agustian, E., Widjaya, R. R., & Dwiatmoko, A. A. (2023). Bentonite pillarization using sonication in a solid acid catalyst preparation for the oleic acid esterification reaction. *Catalysis Communications*, 174, 106598. https://doi.org/10.1016/j.catcom.2022.106598
- Rinaldi, R., & Schüth, F. (2009). Design of solid catalysts for the conversion of biomass. *Energy & Environmental Science*, 2(6), 610– 626. https://doi.org/10.1039/B902668A
- Rodiansono, Trisunaryanti, W., Triyono. 2007. The influence of loading of Ni and Nb_2O_5 to characters of Ni/Zeolite and Ni/Zeolite- Nb_2O_5 catalysts. *Journal of Sains dan Kimia Terapan*, 1, 20-28.
- Salerno, P., Mendioroz, S., & López Agudo, A. (2004). Al-pillared montmorillonite-based NiMo catalysts for HDS and HDN of gas oil: Influence of the method and order of Mo and Ni impregnation. *Applied Catalysis A: General, 259*(1), 17–28. https://doi.org/10.1016/j.apcata.2003.09.019
- Sing, K. S. W., Everett, D. H., Haul, R. A. W., Moscou, L., Pierotti, R. A., Rouquerol, J., & Siemieniewska, T. (2008). Reporting Physisorption Data for Gas/Solid Systems. In G. Ertl, H. Knözinger, F. Schüth, & J. Weitkamp (Eds.), Handbook of Heterogeneous Catalysis (1st ed., pp. 1217–1230). Wiley. https://doi.org/10.1002/9783527610044.hetcat0065
- Sudarma, N., & Parwata, I. M. O. A. (2017). Determination Ethanol In Arak With Gas Chromatography. *Bali Medika Jurnal*, 4(2), 126–135. https://doi.org/10.36376/bmj.v4i2.10

- Sun, J., & Wang, Y. (2014). Recent Advances in Catalytic Conversion of Ethanol to Chemicals. ACS Catalysis, 4(4), 1078–1090. https://doi.org/10.1021/cs4011343
- Sun Kou, M. R., Mendioroz, S., & Muñoz, V. (2000). Evaluation of the Acidity of Pillared Montmorillonites by Pyridine Adsorption. Clays and Clay Minerals, 48(5), 528–536. https://doi.org/10.1346/CCMN.2000.0480505
- Supeno, M., & Siburian, R. (2018). Role of TiO ₂ pillared bentonite-Co catalyst Ni to convert glucose hydrogenation to be sorbitol. *Journal of Physics: Conference Series, 1116,* 042038. https://doi.org/10.1088/1742-6596/1116/4/042038
- Suseno, A. (2019). Hydrocracking of palm oil to gasoline on bimetallic Ni-Cu/zirconia pillared bentonite. IOP Conference Series: Materials Science and Engineering, 509, 012005. https://doi.org/10.1088/1757-899X/509/1/012005
- Thommes, M., Kaneko, K., Neimark, A. V., Olivier, J. P., Rodriguez-Reinoso, F., Rouquerol, J., & Sing, K. S. W. (2015). Physisorption of gases, with special reference to the evaluation of surface area and pore size distribution (IUPAC Technical Report). *Pure and Applied Chemistry*, 87(9–10), 1051–1069. https://doi.org/10.1515/pac-2014-1117
- Wang, F., Kang, X., Zhou, M., Yang, X., Gao, L., & Xiao, G. (2017). Sn and Zn modified HZSM-5 for one-step catalytic upgrading of glycerol to value-added aromatics: Synergistic combination of impregnated Sn particles, ALD introduced ZnO film and HZSM-5 zeolite. Applied Catalysis A: General, 539, 80–89. https://doi.org/10.1016/j.apcata.2017.04.005
- Wen, K., Wei, J., He, H., Zhu, J., & Xi, Y. (2019). Keggin-Al30: An intercalant for Keggin-Al30 pillared montmorillonite. Applied Clay Science, 180, 105203. https://doi.org/10.1016/j.clay.2019.105203
- Widjaya, R. R., Saridewi, N., Putri, A. A., Rinaldi, N., & Dwiatmoko, A. A. (2021). Fe-Cr pillared clay as catalysts for the ethanol to gasoline conversion. *IOP Conference Series: Materials Science and Engineering*, 1011(1), 012008. https://doi.org/10.1088/1757-899X/1011/1/012008
- Widjaya, R. R., Soegijono, B., & Rinaldi, N. (2012). Characterization of Cr/Bentonite and HZSM-5 Zeolite as Catalysts for Ethanol Conversion to Biogasoline. *MAKARA of Science Series*, 16(1). https://doi.org/10.7454/mss.v16i1.1283
- Yanti, F. M., Valentino, N., Juwita, A.R., Murti, S.D., Pertiwi, A., Rahmawati, N., Rini, T.P., Sholihah, A., Prasetyo, J., Saputra, H., Iguchi, S., Noda R. (2020). Methanol production from biomass syngas using Cu/ZnO/Al2O3 catalyst. *AIP Conf. Proc.* 2223, 020006. https://doi.org/10.1063/5.0000870



© 2025. The Author(s). This article is an open access article distributed under the terms and conditions of the Creative Commons Attribution-ShareAlike 4.0 (CC BY-SA) International License (http://creativecommons.org/licenses/by-sa/4.0/)